

Strongly coupled charge-density wave transition in single-crystal $\text{Lu}_5\text{Ir}_4\text{Si}_{10}$

B. Becker, N. G. Patil,* S. Ramakrishnan,* A. A. Menovsky,† G. J. Nieuwenhuys, and J. A. Mydosh
Kamerlingh Onnes Laboratory, Leiden University, 2300 RA Leiden, The Netherlands

M. Kohgi and K. Iwasa

Department of Physics, Tokyo Metropolitan University, Tokyo 192-0397, Japan

(Received 13 November 1998)

We report the observation of a strongly coupled first-order charge-density wave (CDW) transition in a high-quality single crystal of the intermetallic compound $\text{Lu}_5\text{Ir}_4\text{Si}_{10}$. The first-order nature is ascertained by a very narrow and huge cusp (360 J/mol K) in the specific heat. The susceptibility and the resistivity also show sharp jumps at the transition $T_{\text{CDW}}=83$ K. The periodic lattice distortion associated with the CDW is exemplified by the formation of x-ray superlattice reflections along the tetragonal \vec{c} axis with $\vec{q}\approx(0,0,\frac{3}{7})$ ($T<83$ K). Although our results are in accordance with a quasi-one-dimensional CDW scenario, the first-order transition suggests a strong interchain coupling. We propose $\text{Lu}_5\text{Ir}_4\text{Si}_{10}$ as a paradigm of such strong-coupling CDW systems. [S0163-1829(99)05808-7]

The occurrence of charge-density waves (CDW's) in low-dimensional compounds was first addressed by Peierls¹ and Fröhlich,² who showed that a one-dimensional electron gas, coupled to phonons, is unstable at low temperatures against a periodic lattice distortion, which results in a metal-insulator transition. Experimentally, this was initially observed in the platinum chain compound $\text{K}_2\text{Pt}(\text{CN})_4\cdot 0.3\text{Br}\cdot x\text{H}_2\text{O}$,³ and the quasi-one-dimensional (1D) organic charge transfer salt TTF-TCNQ.⁴ The Peierls-Fröhlich theory is a weak electron-phonon coupling approach in the mean-field scenario, which is equivalent to the BCS theory and predicts a second-order phase transition that attributes the formation of CDW's to the reduced dimensionality of the Fermi surface (FS) and its nesting.⁵ However, in the absence of interchain coupling, 1D fluctuations shift the phase transition to 0 K. Finite T_{CDW} is observed only due to a weak 3D coupling between the chains, and the Peierls-Fröhlich transition is strongly reduced below its mean-field value. In some cases, such as in NbSe_3 ,⁶ a substantial transverse coupling has induced a semimetallic behavior. Many predictions for the properties of CDW's, such as nonlinear transport, in systems like quasi-1D NbSe_3 (Ref. 7) or the quasi-1D blue bronzes,⁸ have been experimentally verified. However, the explanation for the thermodynamic properties reflecting the nature of the CDW transition in TaSe_2 (Ref. 9) and the blue bronze $\text{K}_{0.3}\text{MoO}_3$ (Ref. 10) requires a description beyond the weak-coupling theory. The first-order CDW transition in TaSe_2 (Ref. 11) can be semi-quantitatively understood via a microscopic theory proposed by McMillan.¹² This model invokes a short coherence length which leads to significant phonon softening (lattice entropy) as measured by Moncton, Axe, and Di Salvo⁹ at T_{CDW} . The influence of structural defects on the first- or second-order CDW transition is poorly understood, and often complicates the analysis. An experimental search for new strong interchain coupled CDW systems would clearly give a better understanding of CDW behavior.

In this paper we provide an observation of a first-order CDW transition in stoichiometric single crystals of

$\text{Lu}_5\text{Ir}_4\text{Si}_{10}$ at $T_{\text{CDW}}=83$ K. The single-crystal x-ray diffraction confirms the periodic lattice distortion (PLD) by tracking the appearance and growth of superlattice peaks along the tetragonal \vec{c} axis with $\vec{q}\approx(0,0,\frac{3}{7})$ ($T<83$ K). The specific-heat anomaly is sharper than those reported on other CDW systems. We classify $\text{Lu}_5\text{Ir}_4\text{Si}_{10}$ as a strong interchain coupled CDW system with a first-order phase transition.

$\text{Lu}_5\text{Ir}_4\text{Si}_{10}$ adopts a tetragonal $\text{Sc}_5\text{Co}_4\text{Si}_{10}$ ($P4/mbm$) structure, and becomes superconducting below 3.9 K.¹³ From their studies on polycrystalline samples, Shelton *et al.*¹⁴ suggested a partial gapping of the FS which was inferred from the increase of the resistivity and the decrease of susceptibility with decreasing temperature at the phase transition, 80 K. High-pressure studies¹⁵ revealed the progressive suppression to lower temperatures of this transition and its ultimate quenching at 21.4 kbar, with a concomitant rise in the superconducting T_c from 3.9 to 9.1 K. This reflects the intimate interplay of both transitions. Shelton *et al.*¹⁴ claimed the possibility of a CDW formation at 80 K in $\text{Lu}_5\text{Ir}_4\text{Si}_{10}$. However, all of these studies were made of polycrystalline samples, and, thus, contain no information on the anisotropy which is expected for a CDW compound. Moreover, the metallic nature of $\text{Lu}_5\text{Ir}_4\text{Si}_{10}$ is in contrast to the behavior of typical CDW systems. It is worthwhile to recall here that similar anomalies could arise due to Martensitic structural instabilities. As an example, these instabilities in the A15 compounds are attributed to the lifting of the degeneracy of electronic bands.^{16,17} In order to elucidate the properties of $\text{Lu}_5\text{Ir}_4\text{Si}_{10}$ and to prove the existence of the CDW, we have undertaken thermodynamic, transport and low-temperature x-ray-diffraction measurements on single crystals.

Single-crystalline samples have been grown in a tri-arc furnace using a modified Czochralski technique¹⁸ (pulling rate 10 mm/h; seed rotation, 20 rpm for the counter-rotating crucible). The purities of the elements melted in a stoichiometric ratio were Lu: 4N; Ir: 4N; and Si: 5N. Parts of the single crystal have been sealed in a quartz tube, and annealed under high vacuum at 900 °C for one week. All samples

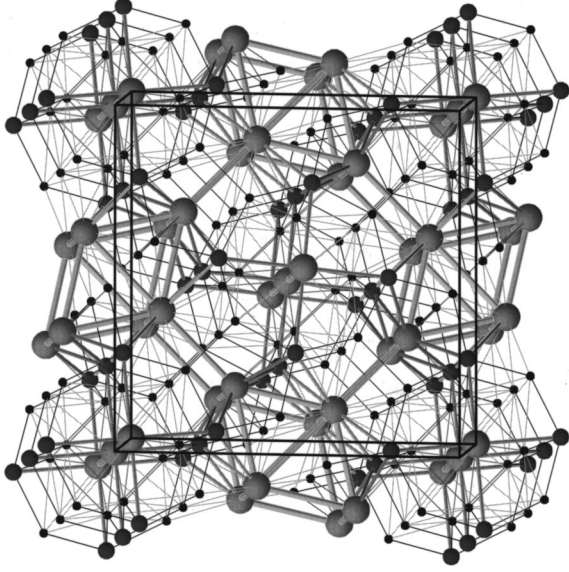


FIG. 1. Crystal structure of tetragonal $\text{Lu}_5\text{Ir}_4\text{Si}_{10}$ ($a = 12.4936 \text{ \AA}$, $c = 4.1852 \text{ \AA}$). Large, intermediate, and small spheres represent Lu, Ir, and Si, respectively. The Lu-Lu bonds shorter than 4.3 \AA are indicated by the thick lines. Lu-Ir bonds have an intermediate thickness, and other bonds shorter than 3.3 \AA are drawn as thin lines.

have been analyzed by electron-probe microanalysis, which proved them to be single phase (second phase $< 1\%$) and to have the correct 5:4:10 stoichiometry (within the 1% resolution). The single crystallinity has been verified by x-ray Laue diffraction. For transport and low temperature magnetization measurements, small bars have been cut by spark erosion from the oriented single crystals.

Figure 1 illustrates the structure of $\text{Lu}_5\text{Ir}_4\text{Si}_{10}$, where long solid lines indicate the tetragonal unit cell. Lu-Lu bonds are shown by thick lines. Atomic positions in the unit cell are refined using a single-crystal x-ray diffractometer with 2642 reflections at 295 K. The estimated positions are given in Table I ($R = 0.05$). $\text{Lu}_5\text{Ir}_4\text{Si}_{10}$ has rather good metallic properties [$\rho(295 \text{ K}) \approx 200 \mu\Omega \text{ cm}$],¹⁵ nevertheless we can assume as in Ref. 7 that the bond length is a qualitative measure for the “metallic” conduction along the bond direction. The Lu atoms occupy three different sites, of which Lu1 has the highest local symmetry with its fourfold axis, and the nearest Lu neighbor of Lu1 lying along the \vec{c} axis (4.1852 \AA). The two Lu1 atoms are connected via short

TABLE I. Atomic positions lengths for $\text{Lu}_5\text{Ir}_4\text{Si}_{10}$ at 295 K. Lattice parameters: $a = 12.4936 \pm 0.0012 \text{ \AA}$ and $c = 4.1852 \pm 0.0006 \text{ \AA}$. x, y , and z are the Cartesian atomic coordinates.

Site	x/a	y/a	z/c
Lu1	0	0	0
Lu2	0.1741(1)	$-x + \frac{1}{2}$	$\frac{1}{2}$
Lu3	-0.1153(1)	$x + \frac{1}{2}$	$\frac{1}{2}$
Ir	0.0187(1)	0.2454(1)	0
Si1	0.0631(9)	$-x + \frac{1}{2}$	0
Si2	0.2003(9)	0.163(1)	0
Si3	0.004(1)	0.156(1)	$\frac{1}{2}$

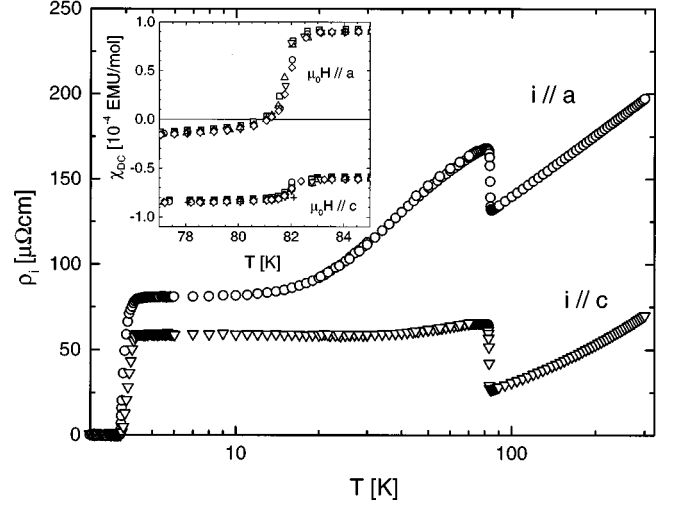


FIG. 2. Resistivity vs temperature of $\text{Lu}_5\text{Ir}_4\text{Si}_{10}$ for $\vec{i} // \vec{a}$ (\circ) and $\vec{i} // \vec{c}$ (∇). Inset: dc susceptibility vs temperature of $\text{Lu}_5\text{Ir}_4\text{Si}_{10}$ in different magnetic fields along the \vec{a} and \vec{c} axes [0.5 T : (\square), 1 T (\circ), 2 T (Δ), 3 T (∇), 4 T (\diamond) and 5 T ($+$)]. The data have been corrected for 50-wt ppm of rare-earth impurities. Note the corrected susceptibility is independent of magnetic field.

bonds to Si3 atoms, and form a chainlike structure along the \vec{c} axis. The Ir atoms separate the Lu1 chains from the Lu2 and Lu3 atoms ($d_{\text{Lu1-Lu2}} = 5.0574 \text{ \AA}$ and $d_{\text{Lu1-Lu3}} = 5.460 \text{ \AA}$). Short Lu-Lu bonds occur between Lu2 and Lu3 sites ($d_{\text{Lu2-Lu3}} = 3.676 \text{ \AA}$). As a first approximation, the structure $\text{Lu}_5\text{Ir}_4\text{Si}_{10}$ can be visualized as 1D chains of Lu1 atoms (bonded to Ir and Si3 atoms) which are embedded in a network of closely bonded Lu2 and Lu3 atoms.

Figure 2 displays the temperature dependence of resistivity (ρ) along the \vec{a} and \vec{c} axes. At 300 K the resistivity values are $\rho_a \approx 195 \mu\Omega \text{ cm}$ and $\rho_c \approx 60 \mu\Omega \text{ cm}$. The $\rho(T)$ data show a sharp upward jump at 83 K ($\Delta\rho \approx 30 \mu\Omega \text{ cm}$ with $\Delta T \leq 1.5 \text{ K}$) with decreasing temperature. The sample undergoes a superconducting transition at 3.9 K with a width (10–90%) of $\pm 0.1 \text{ K}$. The inset of Fig. 2 shows the dc susceptibility, which is anisotropic, and exhibits a sharp drop as the temperature is decreased below T_{CDW} . The jump sizes are $\Delta\chi_a = 1 \times 10^{-4} \text{ emu/mol}$ and $\Delta\chi_c = 0.24 \times 10^{-4} \text{ emu/mol}$ for magnetic fields along the \vec{a} and \vec{c} axes, respectively.

Heat-capacity measurements have been performed using a quasiadiabatic heat pulse technique. The temperature dependence of the specific heat (c_p) plotted in Fig. 3 shows a huge spike ($\Delta c_p \approx 160 \text{ J/mol K}$) at T_{CDW} . The transition is accompanied by an entropy change of $0.5R$ where R is the gas constant. The height of the peak in $c_p(T)$ indicates a first-order phase transition.

Single-crystal x-ray diffraction has been measured at 10 K by performing $(h, 0, \xi)$ scans with $h = 0, 1, 2, 3$. No temperature dependence of the structural ($P4/mbm$) peak intensity was observed. X-ray superlattice peaks appear below 85 K, which can be indexed as $[h, 0, l + (n/7)]$, where $n = 1, 2, \dots, 6$. The relative intensities of the superlattice peaks depend on the scans; however, among these the largest in-

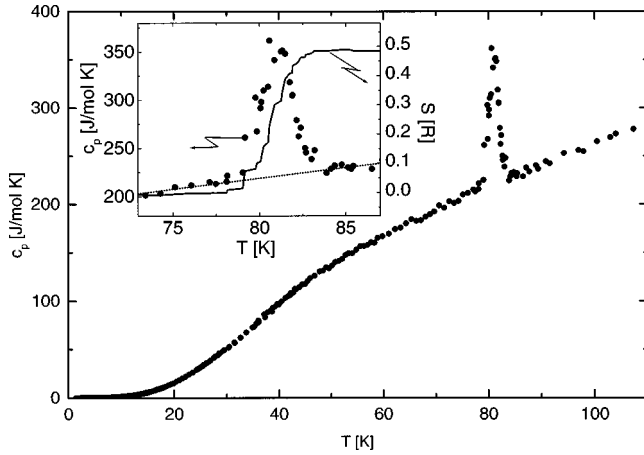


FIG. 3. Specific heat vs temperature of $\text{Lu}_5\text{Ir}_4\text{Si}_{10}$. Inset: Specific heat on an enlarged temperature scale with linear fit to “background” (left axis), and calculated entropy change after the subtraction of the “background” around 83 K (right axis).

intensities are observed for the $(h,0,l \pm \frac{3}{7})$ peaks. Figure 4 exhibits the temperature dependence of the superlattice peak intensity as observed in $(0,0,\xi)$ scans. The position of the two superlattice peaks, corresponding to the Mo $K_{\alpha 1}$ and Mo $K_{\alpha 2}$ lines, do not shift with respect that of structural ($P4/mbm$) peaks with temperature. This implies that \vec{q} is along the \vec{c} direction and is T independent. The inset of Fig. 4 shows the temperature dependence of the integrated intensities. At 80 K nearly the full integrated superlattice peak intensity is attained.

The appearance of the superlattice reflections at $[h,0,l + (n/7)]$ firmly establishes the PLD with a commensurate lattice modulation of seven ($P4/mbm$) unit cells. The largest $(h,0,l \pm \frac{3}{7})$ superlattice peak intensities indicate $\vec{q} \approx (0,0,\frac{3}{7})$. Nevertheless, the actual structural modulation is not simply a sine wave because of the presence of all the components of

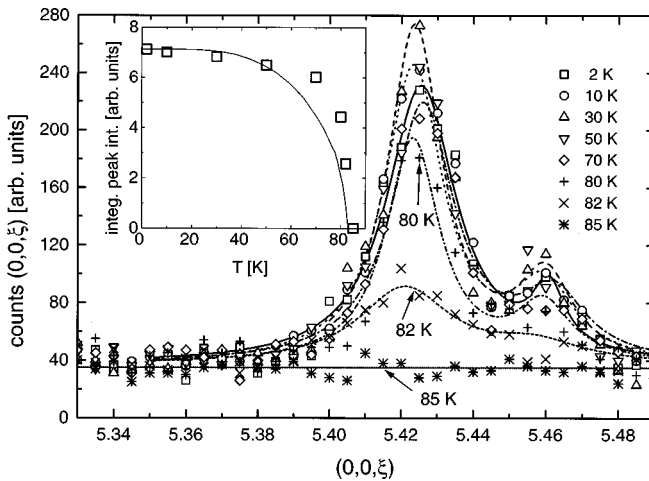


FIG. 4. X-ray-diffraction pattern of the superlattice reflections peaks of $\text{Lu}_5\text{Ir}_4\text{Si}_{10}$ at different temperatures. The lines indicate the best fit to two Lorentzian lines. The inset: Integrated peak intensities vs temperature of the superlattice reflections of $\text{Lu}_5\text{Ir}_4\text{Si}_{10}$ calculated from the best fits to the two Lorentzian lines. For comparison, the solid line represents the temperature dependence of the BCS gap.

the superlattice modulation with a seven-unit-cell period along the \vec{c} axis. A lattice modulation along the \vec{c} axis implies a quasi-1D PLD, and excludes a structural transition driven by a lifting of an electronic band degeneracy.¹⁷ The occurrence of the superlattice peaks at 2 K demonstrates the coexistence of CDW's and superconductivity, which will be discussed elsewhere.¹⁹

The magnetic susceptibility can be expressed as $\vec{\chi}_i = \vec{\chi}_C + \vec{\chi}_P + \vec{\chi}_{i,L}$, where $\vec{\chi}_C$ is the isotropic core susceptibility, $\vec{\chi}_P$ is the isotropic Pauli susceptibility, and $\vec{\chi}_{i,L}$ is the anisotropic Landau susceptibility. The direction of the magnetic field is indicated by i ($\vec{B} // \vec{a}$ or $\vec{B} // \vec{c}$). $\vec{\chi}_{i,L}$ can be calculated from the band structure,²⁰ which is unfortunately not known at the present. However, the anisotropic susceptibility implies an anisotropic FS. The drop of $\chi(T)$ at T_{CDW} corresponds to a change of the density of states at the FS. The reduced drop along the \vec{c} axis is consistent with the model of Boriack²¹ which predicted a smaller Landau (negative) contribution of the FS along the chain direction as compared to that perpendicular to the \vec{c} axis.

The absence of a metal-insulator transition at T_{CDW} implies a partial gapping of the FS. Furthermore, for typical CDW systems the anisotropy in ρ , measured as the ratio parallel and perpendicular to the chain direction, is much larger²² than observed for $\text{Lu}_5\text{Ir}_4\text{Si}_{10}$. The behavior of $\rho_c(T)$ can be qualitatively understood within a simple model assuming two conductivity channels, one related to the Lu1 chains and the other due to the Lu2-Lu3 network. The first channel at T_{CDW} undergoes a metal-insulator transition, while the network remains metallic. The projection of the FS change on the \vec{a} axis governs $\rho_a(T)$, thereby giving the step at T_{CDW} .

Although the resistivity and the susceptibility can be understood within a conventional CDW scenario, the large anomaly in the specific heat makes this CDW transition especially unusual. Most of the CDW systems have only small c_p anomalies at their T_{CDW} .²³ They also have a significant excess specific heat associated with the fluctuations of the order parameter in the region spanning 5–10 % of the reduced temperature $[(T - T_{\text{CDW}})/T_{\text{CDW}}]$. In contrast, to the best of our knowledge, $\text{Lu}_5\text{Ir}_4\text{Si}_{10}$ exhibits the sharpest cusp observed in any reported CDW system with $\Delta T/T_{\text{CDW}} \approx 1\%$. It has been suggested²⁴ that defects, etc., eliminate the critical cusp, leaving milder corrections to the scaling cusp. Clearly, defects seem to play a minor role in $\text{Lu}_5\text{Ir}_4\text{Si}_{10}$. Our semiadiabatic technique restricts the analysis of the sharpness of the transition to $\Delta T/T_{\text{CDW}} \approx 0.5\%$.

The temperature dependence of the x-ray peak intensities distinctly shows a non-BCS-like dependence for the CDW order parameter, indicating the nonapplicability of the Peierls-Fröhlich theory. McMillan¹² proposed that when the coherence length of the CDW state is short, the lattice plays a dominant role in the thermodynamics of the CDW transition with a strong critical behavior. A large phonon contributions to c_p could arise from phonon softening that results in the Kohn anomaly.⁹ In the weak-coupling limit (diverging coherence length at T_{CDW}) the energy gap Δ corresponds to the BCS expression $\Delta(0\text{K}) = 3.53k_B T_c$. In order to apply McMillan's short coherence length model, one must have

$\Delta(0) > 7k_B T_{CDW}$. Preliminary measurements²⁵ of the optical reflectivity show a change in the spectral weight as a function of temperature below 500 cm^{-1} which indicates charge (and structural) fluctuations with an increased number of carriers for $T > T_{CDW}$. A gap of order 700 K ($\approx 500 \text{ cm}^{-1}$) is in agreement with the prerequisites of the McMillan model. A qualitative description of $\text{Lu}_5\text{Ir}_4\text{Si}_{10}$ within the later theory seems possible.

In the case of blue bronze Kwok, Gruner, and Brown¹⁰ discussed their results in terms of McMillan's model, although the changes in the Young's moduli²⁶ are small (2–3 %). The analysis of the critical exponents²⁶ shows deviations from the predictions of a CDW transition in a quasi-1D metal²⁷ due to defects wiping out the critical cusp in the specific heat. Here weak pretransition fluctuations have been observed in x-ray scattering experiments,⁸ although they are strongly reflected in transport and thermodynamic data.^{10,26} In $\text{Lu}_5\text{Ir}_4\text{Si}_{10}$, no indications of pretransition fluctuations are evident from our x-ray, thermodynamic, and transport studies. Note, e.g., in Fig. 4 at 85 K, the absence of such (broad) superlattice reflection within the resolution. For a quasi-1D CDW one would expect strong fluctuations above T_{CDW} . However, strong coupling between the chains would make the problem more 3D and therefore suppress these

fluctuations. Such strong coupling is not included in McMillan's theory.¹² The absence or weakness of precursor effects indicates strong interchain coupling in $\text{Lu}_5\text{Ir}_4\text{Si}_{10}$. Furthermore, in this stoichiometric single crystals defects seem to play a minor role as compared to the blue bronzes. A new theoretical description beyond the McMillan model is required to understand the unusual CDW properties of $\text{Lu}_5\text{Ir}_4\text{Si}_{10}$.

To conclude, detailed bulk measurements along with x-ray studies suggest a strong interchain coupled first-order CDW transition below 83 K in $\text{Lu}_5\text{Ir}_4\text{Si}_{10}$ single crystals. This material could serve as a prototype for strong interchain coupled quasi-one-dimensional CDW systems. Further experimentation on $\text{Lu}_5\text{Ir}_4\text{Si}_{10}$, concerning the structural fluctuations (synchrotron radiation) and the lattice softening (inelastic neutron scattering), would lead to a better understanding of CDW's beyond the weak-coupling limit. Finally, there exists a series of magnetic rare earth 5-4-10 allomorphs²⁸ that allow new investigations of the coexistence and/or competition of magnetism and CDW.

This work was supported in part by the Dutch Stichting FOM. We wish to acknowledge S. Gorter for structure refinements, and many fruitful discussions with J. Zaanen.

*Permanent address: Tata Institute of Fundamental Research, Mumbai-400005, India.

[†]Also at Van der Waal Zeeman Laboratory, University of Amsterdam, The Netherlands.

¹R. E. Peierls, *Quantum Theory of Solids* (Oxford University Press, London, 1955), p. 108.

²H. Fröhlich, Proc. R. Soc. London, Ser. A **223**, 296 (1954).

³See e.g., R. Comes, M. Lambert, H. Launois, and H. R. Zeller, Phys. Rev. B **8**, 571 (1973).

⁴L. B. Coleman, M. J. Cohen, D. J. Sandman, F. G. Yamagishi, A. F. Garito, and A. J. Heger, Solid State Commun. **12**, 1125 (1973).

⁵J. P. Pouget, in *Low-Dimensional Electronic Properties of Molybdenum Bronzes and Oxides*, edited by C. Schlenker (Kluwer, Dordrecht, 1989), p. 87.

⁶J. P. Sorbier, H. Tortel, P. Monceau, and F. Levy, Phys. Rev. Lett. **76**, 676 (1996).

⁷N. P. Ong and P. Monceau, Phys. Rev. B **16**, 3443 (1977); N. P. Ong and J. W. Brill, *ibid.* **18**, 5265 (1978).

⁸S. Girault, A. H. Moudden, and J. P. Pouget, Phys. Rev. B **39**, 4430 (1989).

⁹D. E. Moncton, J. D. Axe, and F. J. DiSalvo, Phys. Rev. Lett. **34**, 734 (1975); Phys. Rev. B **16**, 801 (1977).

¹⁰R. S. Kwok, G. Gruner, and S. E. Brown, Phys. Rev. Lett. **65**, 365 (1990).

¹¹J. A. Wilson, F. J. DiSalvo, and S. Mahajan, Adv. Phys. **24**, 117 (1975).

¹²W. L. McMillan, Phys. Rev. B **16**, 643 (1977).

¹³H. F. Braun, Acta Crystallogr., Sect. B: Struct. Crystallogr. Cryst.

Chem. **36**, 2397 (1980); J. Less-Common Met. **100**, 105 (1984).

¹⁴R. N. Shelton, L. S. Hausermann-Berg, P. Klavins, H. D. Yang, M. S. Anderson, and C. A. Swenson, Phys. Rev. B **34**, 4590 (1986).

¹⁵H. D. Yang, R. N. Shelton, and H. F. Braun, Phys. Rev. B **33**, 5062 (1986).

¹⁶M. Weger and I. B. Goldberg, in *Solid State Physics*, edited by H. Ehrenreich, F. Seitz, and D. Turnbull (Academic, New York, 1973), Vol. 28, p. 1.

¹⁷G. Bilbro and W. L. Mc Millan, Phys. Rev. B **14**, 1887 (1976).

¹⁸A. A. Menovsky and J. J. M. Franse, J. Cryst. Growth **65**, 286 (1983).

¹⁹B. Becker, Ph.D. thesis, Leiden University, 1998.

²⁰P. K. Misra and L. M. Roth, Phys. Rev. **177**, 1089 (1969).

²¹M. L. Boriack, Phys. Rev. Lett. **44**, 208 (1980).

²²C. Schlenker, J. Dumas, C. Escribe-Filippini, and H. Guyot, in *Low-Dimensional Electronic Properties of Molybdenum Bronzes and Oxides*, edited by C. Schlenker (Kluwer, Dordrecht, 1989), p. 159.

²³For instance, $\Delta S = 0.03R$ for TTF-TCNQ with $[\Delta T/T_{CDW}] = 10\%$, whereas for $\text{K}_{0.3}\text{MoO}_3$, the corresponding values are 0.11R and 7%. See also Ref. 20.

²⁴J. A. Aronovitz, P. Goldbart, and G. Mozurkewich, Phys. Rev. Lett. **64**, 2799 (1990).

²⁵A. Damascelli (private communication).

²⁶J. W. Brill, M. Chung, Y. K. Kuo, X. Zhan, E. Figueroa, and G. Mozurkewich, Phys. Rev. Lett. **74**, 1182 (1995).

²⁷Z. Y. Chen, Phys. Rev. B **41**, 9516 (1990).

²⁸H. D. Yang, P. Klavins, and R. N. Shelton, Phys. Rev. B **43**, 7688 (1991).